UC Davis
UC Davis Previously Published Works

Title

Tethered bis-pyrrolidine additions to C70: Some unexpected and new regioisomers

Permalink

https://escholarship.org/uc/item/9s5760bf

Authors

Cerón, Maira R
Izquierdo, Marta
Aghabali, Amineh
et al.

Publication Date

2016-08-01

DOI

10.1016/j.carbon.2016.04.044

Peer reviewed

Contents lists available at ScienceDirect

Carbon

CrossMark

Tethered *bis*-pyrrolidine additions to C_{70}: Some unexpected and new regioisomers

Maira R. Cerón [a, 1], Marta Izquierdo [a, 1], Amineh Aghabali [b, 1], Sophie P. Vogel [a], Marilyn M. Olmstead [b, ***], Alan L. Balch [b, **], Luis Echegoyen [a, *]

[a] Department of Chemistry, University of Texas at El Paso, 500W University Ave, El Paso, TX 79968, USA
[b] Department of Chemistry, University of California at Davis, One Shields Ave, Davis, CA 95616, USA

ARTICLE INFO

ABSTRACT

Four easily isolable *bis*-pyrrolidine-C_{70} regioisomers were synthesized and characterized by spectroscopic techniques. The four [70]fullerene *bis*-adducts were unambiguously assigned using spectroscopic techniques and X-ray crystallography, as the β-2-β, α-2-α, α-1-β and α-1-α regioisomers.

© 2016 Elsevier Ltd. All rights reserved.

1. Introduction

Fullerene derivatives have been extensively used as electron acceptor materials in organic photovoltaic (OPV) solar cells [1–3]. Currently [6,6]-phenyl-C_{61}-butyric acid methyl ester ($PC_{61}BM$) is widely used in OPV solar cells [2,4–8]. Recently, considerable effort has been devoted to the search for other fullerene-based compounds with optimal performance in OPV solar cells [2,4–8]. As a result, it has been shown that [70]fullerene *bis*-adducts exhibit appealing acceptor properties partly due to the higher absorption coefficient of C_{70} compared with that of C_{60}, and the higher lowest unoccupied molecular orbital (LUMO) levels compared with those of monoadduct analogs [2,9–11]. It was also demonstrated that the use of some regioisomerically pure *bis*-adducts resulted in higher efficiencies compared with those of the corresponding isomeric mixtures [9,11–15]. However, impractical and time-consuming techniques are usually required for the purification of *bis*-adduct regioisomers [16]. Thus, there is a need to develop selective reactions that are able to efficiently produce pure fullerene *bis*-adduct regioisomers to avoid high-performance liquid chromatography (HPLC) separations. A pioneer in this field was Diederich and co-workers who introduced the tether-directed remote multi-functionalization, which involved the addition of two or more reactive centers linked by a spacer of a given length and rigidity [17–19].

The chemical reactivity of higher fullerenes such as C_{70}-D_{5h} has not been fully investigated mainly because of its lower symmetry compared with that of C_{60}-I_h, which results in an increase of the number of isomers observed. C_{70} possesses four inequivalent types of [6,6]-ring junctions defined as α, β, γ and δ (Fig. 1). The strain of these bonds typically determines the most favored sites for additions. The α-bonds, which are the most strained and on the poles of the molecule, are the most reactive bonds, followed by the β- and then the γ-bonds. The δ-bonds, on the equator, are the least reactive.

The most common reactions used to functionalize C_{70} are the [2 + 1], [3 + 2], [2 + 2] or Diels−Alder cycloadditions, which normally give rise to the α-isomer as the major product [20–23]. The 1,3-dipolar cycloaddition of azomethine ylides is the least regioselective reaction, which leads to α, β and γ-isomers in different ratios depending on the reaction conditions and the nature of the azomethine ylide [22,24–28].

Echegoyen *et al.* recently reported some regioselective tethered *bis*-1,3-dipolar cycloadditions on C_{60} and the formation of two regioisomeric *bis*-adducts (*cis*-1 and *cis*-2) out of the 8 possible isomers [29]. The number of possible independent *bis*-adducts on C_{70} is 38 if both addends are identical and additions occur exclusively on [6,6]-bonds. To the best of our knowledge, there is no precedent of *bis*-pyrrolidine additions on C_{70} besides those obtained as byproducts [30]. Due to the difference in symmetry and reactivity of C_{70} compared with C_{60}, it is not possible to predict if using the same tethered reagents will lead to similar regioisomers as observed for C_{60} [29]. Here we report the one step synthesis of
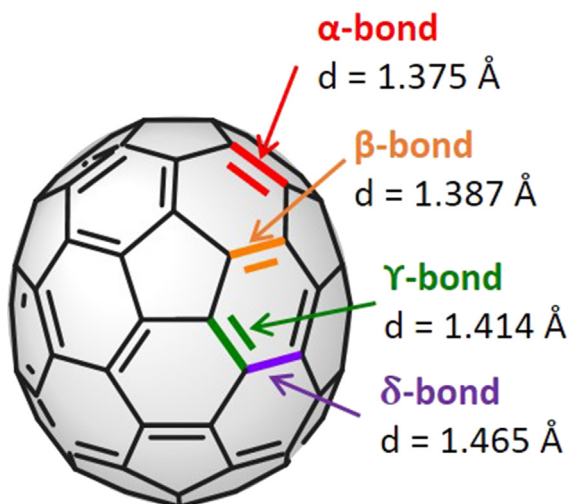
* Corresponding author.
** Corresponding author.
*** Corresponding author.
E-mail addresses: mmolmstead@ucdavis.edu (M.M. Olmstead), albalch@ucdavis.edu (A.L. Balch), echegoyen@utep.edu (L. Echegoyen).
[1] These authors contributed equally.

Fig. 1. Four different reactive [6,6]-bonds of C_{70} [20]. (A colour version of this figure can be viewed online.)

four new *bis*-pyrrolidine C_{70} regioisomers and their full characterization including the X-ray crystal structures of three of them.

2. Experimental

2.1. Synthesis of bis-pyrrolidines C_{70}

Four *bis*-pyrrolidine C_{70} compounds (defined as **1** to **4**) were synthesized following the same procedure described previously by us but using C_{70} instead of C_{60} (Fig. 2) [29]. A mixture of 50.00 mg of C_{70} (0.059 mmol, 1 equiv), 7.98 mg of OPA (0.059 mmol, 1 equiv) and 49.08 mg of *N*-Ethylglycine (0.476 mmol, 8 equiv) in 40 mL of toluene were refluxed for 1 day. After cooling to room temperature, the solvent was removed under vacuum and the crude product was purified by silica gel column chromatography using CS_2 as eluent to recover the unreacted C_{70}, and CS_2:$CHCl_3$ to elute compounds **1** (12% yield) and **2** (23% yield) in order of polarity. By increasing the polarity of the solvents, minor fractions of two additional *bis*-adducts **3** (3% yield) and **4** (3% yield) and of some polyadducts were eluted.

2.2. ^1HNMR chemical shifts of bis-pyrrolidines C_{70}

Compound **1**: δ 7.35 (dd, $1H_{Ar}$, $J = 3.61$, 5.64), 7.07 (dd, $1H_{Ar}$, $J = 3.49$, 5.77), 4.60 (d, 1H, $J = 10.19$), 4.21 (s, 1H), 3.68 (d, 1H, $J = 10.22$), 3.37 (m, 1H, N−C$\underline{H}_2$−CH$_3$, $J = 7.56$, 12.48), 2.35 (m, 1H, N−C$\underline{H}_2$−CH$_3$, $J = 6.91$, 13.87), 1.39 (t, 1H, N−CH$_2$−C$\underline{H}_3$, $J = 7.24$) ppm.
Compound **2**: δ 7.89 (dd, $1H_{Ar}$, $J = 3.71$, 5.47), 7.54 (dd, $1H_{Ar}$, $J = 3.44$, 5.67), 4.74 (d, 1H, $J = 9.92$), 4.10 (s, 1H), 3.60 (m, 1H, N−C$\underline{H}_2$−CH$_3$, $J = 7.38$, 14.90), 3.40 (d, 1H, $J = 9.85$), 2.38 (m, 1H, N−C$\underline{H}_2$−CH$_3$, $J = 6.96$, 13.90), 1.53 (t, 1H, N−CH$_2$−C$\underline{H}_3$, $J = 7.22$) ppm.

2.3. Crystal data for bis-pyrrolidines C_{70} β-2-β (**1**)·toluene

$C_{91}H_{28}N_2$ $M = 1149.15$, black block, $1.155 \times 0.554 \times 0.172$ mm, λ = 0.71073 Å (Bruker ApexII), monoclinic, space group $P2_1/m$ (no. 11), $a = 13.1366(13)$, $b = 13.4026(14)$, $c = 14.5370(15)$ Å, $β = 109.5768(14)$ °, $T = 90(2)$ K, $V = 2411.5(4)$ Å^3, $Z = 2$, 38827 reflections measured, 7640 unique ($R_{int} = 0.0187$) which were used in all calculations, $2θ_{max} = 61.958°$; min/max transmission = 0.7012/0.7462 (multi-scan absorption correction

applied); direct and Patterson methods solution; full-matrix least squares based on F^2 (SHELXT and SHELXL-2014); The final $wR(F_2)$ was 0.1478 (all data), conventional $R_1 = 0.0540$ computed for 6863 reflections with I > 2σ(I) using 438 parameters with no restraints.

2.4. Crystal data for bis-pyrrolidines C_{70} α-1-β (**3**)·CS$_2$

$C_{85}H_{20}N_2S2$, $M = 1114.12$, black block, $0.313 \times 0.188 \times 0.074$ mm, λ = 1.54178 Å (Bruker ApexDuo), orthorhombic, space group *Pbca* (no. 61), $a = 19.4120(6)$, $b = 18.0214(5)$, $c = 26.1217(7)$ Å, $T = 90(2)$ K, $V = 9138.2(5)$ Å^3, $Z = 8$, 37918 reflections measured, 7505 unique ($R_{int} = 0.0516$) which were used in all calculations, $2θ_{max} = 127.36°$; min/max transmission = 0.6234/0.7531 (multi-scan absorption correction applied); direct and Patterson methods solution; full-matrix least squares based on F^2 (SHELXT and SHELXL-2014); The final $wR(F_2)$ was 0.2703 (all data), conventional $R_1 = 0.0899$ computed for 5399 reflections with I > 2σ(I) using 804 parameters with no restraints.

2.5. Crystal data for bis-pyrrolidines C_{70} α-1-α (**4**)·0.4CH$_2$Cl$_2$·CH$_3$OH

$C_{85}H_{22}N_2ClO$, $M = 1103.40$, black block, $0.308 \times 0.278 \times 0.072$ mm, λ = 1.54178 Å (Bruker ApexDuo), orthorhombic, space group *Pbca* (no. 61), $a = 18.9405(9)$, $b = 17.5667(8)$, $c = 27.2806(14)$ Å, $T = 90(2)$ K, $V = 9076.9(8)$ Å^3, $Z = 8$, 49150 reflections measured, 8022 unique ($R_{int} = 0.0612$) which were used in all calculations, $2θ_{max} = 125.46°$; min/max transmission = 0.5889/0.7537 (multi-scan absorption correction applied); direct and Patterson methods solution; full-matrix least squares based on F^2 (SHELXT and SHELXL-2014). The final $wR(F_2)$ was 0.3353 (all data), conventional $R_1 = 0.1187$ computed for 6110 reflections with I > 2σ(I) using 808 parameters with 3 restraints.
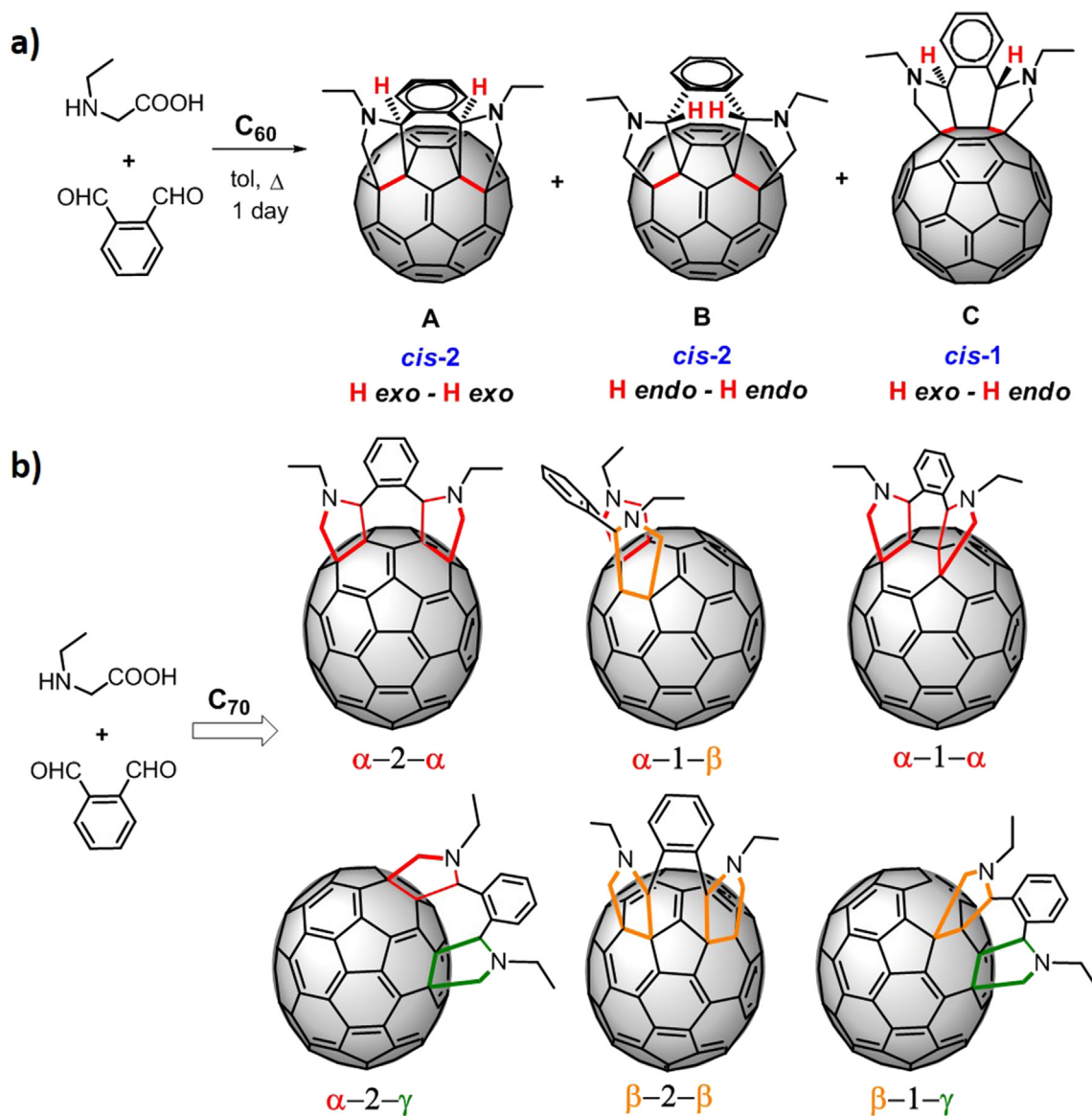
3. Results and discussion

Based on the stereochemical information from the analogous reaction on C_{60} [29], the possible regioisomers that could be obtained with C_{70} are shown in Fig. 2. To determine the number of possible regioisomers on C_{70}, several factors were considered:

i. The *bis*-1,3-dipole should cyclo-add to the most reactive bonds, thus excluding possible combinations such as γ-γ, γ-δ or δ-δ.
ii. The optimal length between the attached addends should be one or two bonds (preferentially two bonds based on the observations with C_{60}).
iii. The stereo-conformation of the hydrogen atoms of both C2 carbons of the pyrrolidine rings can be *endo−endo*, *exo−exo*, *endo-exo* or *exo-endo* and some of these would exist as enantiomeric pairs (Fig. 3).

The tether-controlled multifunctionalization method significantly decreases the number of regioisomers that are likely to form. Nevertheless, due to the reactivity difference of the [6,6]-bonds, the presence of two chiral centers in the addend and the relatively low regioselectivity of the 1,3-dipolar cycloaddition on C_{70}, the number of possible isomers is considerably higher than for C_{60}. For each *site*-isomer (Fig. 2b) three *stereo*-conformations are possible, so a total of 18 possible isomers could be observed.

3.1. Structural characterization of symmetric bis-pyrrolidines C_{70} **1** and **2**

Compounds **1** and **2** were characterized by UV/vis and nuclear

Fig. 2. a) Previously reported *bis*-pyrrolidine C$_{60}$ regioisomers [29]. b) Possible *bis*-pyrrolidine C$_{70}$ *site*-isomers (*site*-isomer refers to the *site* where the additions are placed). *Bis*-adduct regioisomers of C$_{70}$ are named following a recently reported nomenclature [31]. (A colour version of this figure can be viewed online.)

magnetic resonance spectroscopy (NMR), mass spectrometry, and cyclic voltammetry (see ESI). The matrix-assisted laser desorption/ionization time-of-flight (MALDI-TOF) mass spectra confirmed the presence of the molecular-ion peak for the *bis*-adduct products (*m/z* 1056.2120 and 1056.0857 for compounds **1** and **2**, respectively).

The ^{1}H NMR spectra of **1** and **2** exhibit only one set of signals, clearly establishing the presence of a plane of symmetry in each molecule (Fig. 4). These additions must have occurred on the same type of bond (α-α or β-β), because a combination of different types of bonds would result in the formation of unsymmetric products (α-β, α-γ or β-γ). Furthermore, the hydrogen atoms on the stereogenic centers (C2 of the pyrrolidine ring) need to be oriented in the same direction. Thus, the stereo-conformation is either *endo*−*endo* or *exo*−*exo*. The two stereogenic centers in the molecule and the plane of symmetry indicate that compounds **1** and **2** are non-chiral molecules and correspond to a *meso* form. The ^{1}H NMR spectra of **1** and **2** exhibit one singlet in the middle of the AB quartet due to the pyrrolidine protons. Based on this pattern, the chemical shift of the signals and by comparison to the previously reported ^{1}H NMR

spectrum of compound **B** (Fig. 2a, *cis*-2 H *endo*- H *endo*) [24,29,32], we suggest that compounds **1** and **2** exhibit the same *endo*−*endo* conformation.

UV/vis spectroscopy is a useful tool to assign fullerene isomers since unique absorption patterns are observed for each derivative based on the addition sites and not on the nature of the addends. Unfortunately, there are only a few examples of well characterized [70]fullerene *bis*-adducts that have been reported, so assignments based exclusively on the UV/vis absorption spectra are not possible for the most part. Indeed, except for a very few examples [31,33], the reported [70]fullerene *bis*-adducts correspond to double additions on opposite poles of the C$_{70}$ cage [20,34−38].

As discussed before, two bonds between the addition sites are more energetically favorable than one, thus we can reduce the number of possible symmetric regioisomers to α-2-α or β-2-β. To confirm that our hypothesis was correct, we compared the UV/vis spectra of compounds **1** and **2** with that for a previously reported α-1-α (Fig. 5) and by elimination conclude that compounds **1** and **2** are the α-2-α and β-2-β regioisomers. Since compound **2** is the
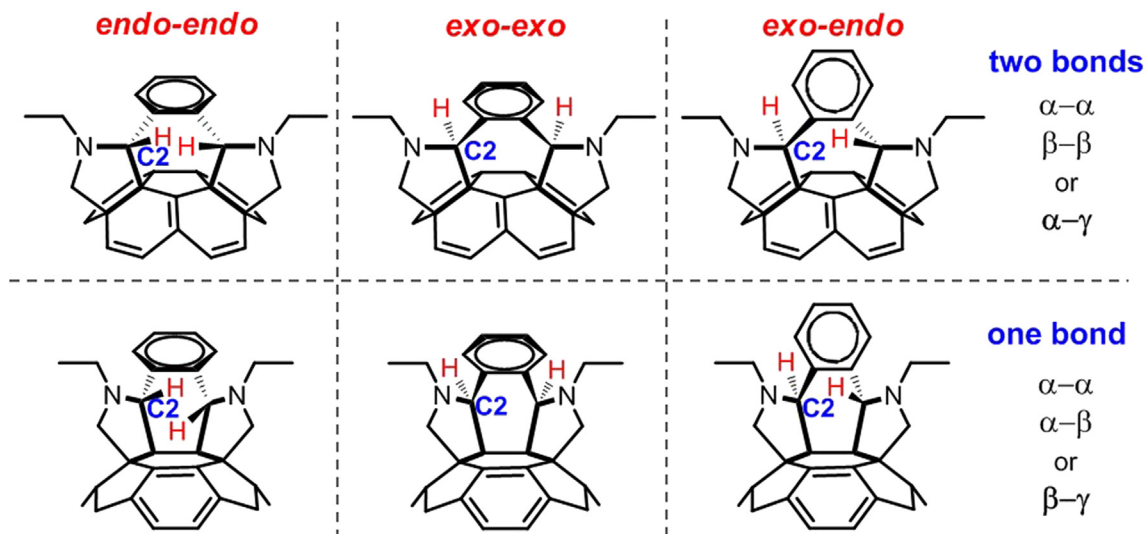
Fig. 3. Stereo-conformation of hydrogens on the C2 of the pyrrolidine ring. (A colour version of this figure can be viewed online.)
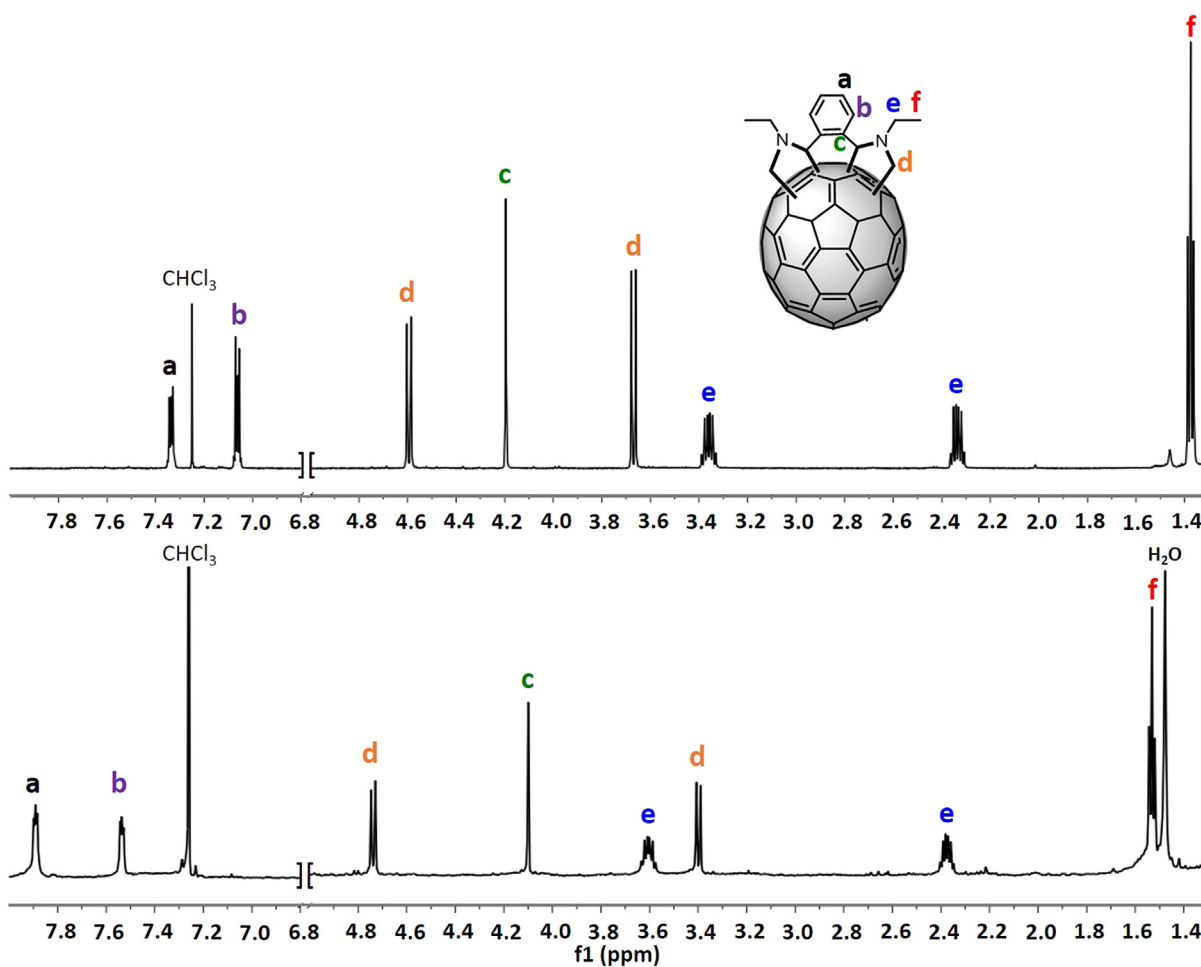

Fig. 4. ^{1}HNMR spectrum of compound **1** (top) and compound **2** (bottom) (600 MHz, 298 K, CS$_2$:CDCl$_3$ 1:1). (A colour version of this figure can be viewed online.)

major product, and the α-2-α regioisomer should be preferred, **2** is assigned as the α-2-α isomer. Therefore, compound **1** is assigned as the β-2-β regioisomer.

Fortunately, crystals of compound **1** were grown by slow evaporation of a toluene solution of the compound. The structure of **1** was determined by X-ray crystallography as shown in Fig. 6. The fullerene is ordered. The asymmetric unit contains half of the adduct with the other half generated by reflection through a
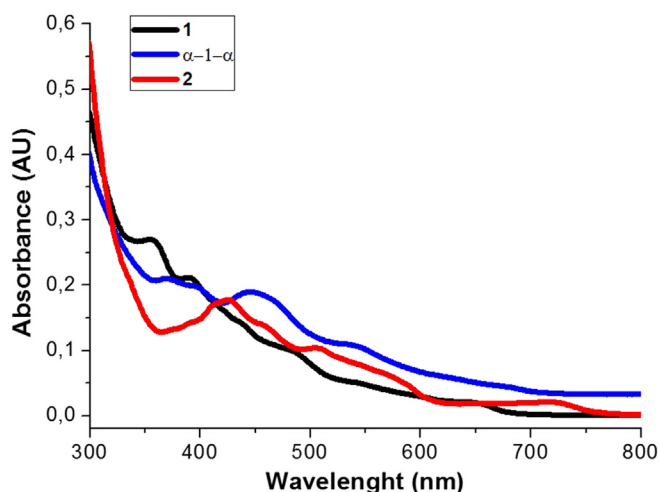
Fig. 5. UV/vis spectra of compounds **1** and **2** compared with the reported α-1-α [31]. (A colour version of this figure can be viewed online.)

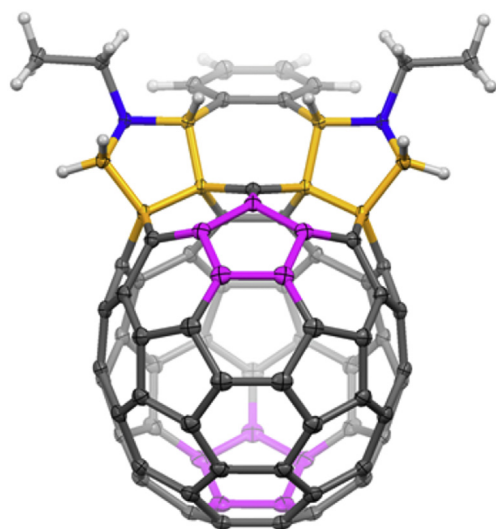**Fig. 6.** Crystallographically determined structure of compound **1** (*meso*-β-2-β *endo-–endo*) from the solvate, **1**•toluene. The apical pentagons of C_{70} are shown in pink and the pyrrolidine rings attached to the β-bonds are yellow. Nitrogen atoms are blue. Thermal ellipsoids are drawn at the 0.50 level. (A colour version of this figure can be viewed online.)

crystallographic mirror plane. Thus compound **1** is the β-2-β regioisomer. The hydrogen atoms at the C2 of the pyrrolidine rings are in an *endo–endo* orientation.

Addition to the cage results in elongation of the C–C bonds

where the adduct forms as shown by the data in Table 1. Little change in distance occurs for the other α- and β-C–C bonds. The pyramidalization of the carbon atoms at the addition sites also increases.

3.2. Structural characterization of unsymmetric bis-pyrrolidines C_{70} 3 and 4

These results establish the structure of compound **1** as the β-2-β regioisomer and thus indicate that compound **2** is likely to be the α-2-α regioisomer. Unfortunately, suitable crystals of compound **2** could not be obtained for X-ray diffraction studies.

A minor fraction of a mixture of [70]fullerene *bis*-adducts **3** and **4** (6% yield) was further purified by recycling HPLC using a Buckyprep column and characterized by UV/vis, NMR spectroscopy and mass spectrometry (see ESI). The ^{1}H NMR spectra of compounds **3** and **4** exhibited no symmetry (see ESI), thus assigning specific regioisomeric structures is very difficult because there are many unsymmetric possibilities, including the α-1-α, α-2-α or β-2-β regioisomers with *endo-exo* stereo-conformations at the C2 positions, or α-1-β, α-2-γ or β-1-γ regioisomers with any of the possible stereo-conformations of the hydrogens. Compounds **3** and **4** showed similar UV/vis absorption spectra to that reported for the α-1-β and α-1-α regioisomers [32], respectively (see ESI) [31].

Crystals of compound **3** were grown by slow diffusion of methanol into a carbon disulfide solution of the adduct. Solution of the structure unambiguously showed that compound **3** is the α-1-β regioisomer (Fig. 7a), with the hydrogen atoms at the C2 positions on the pyrrolidine ring in an *endo-exo* orientation. The molecule crystallizes in a centrosymmetric space group with one entire molecule in the asymmetric unit. Compound **3** is a chiral molecule but the crystal consists of a racemic mixture (*RR* and *SS*), similar to the situation observed for the corresponding C_{60} adduct (compound **C**, Fig. 2a) [29].
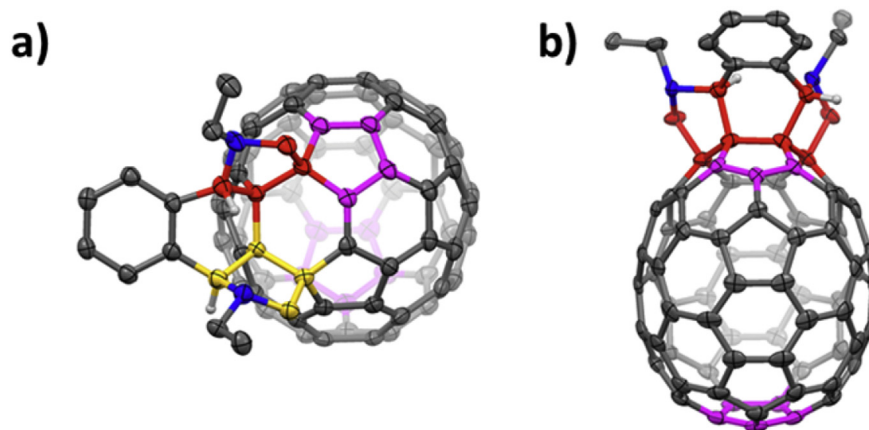
Crystals of compound **4** were grown by slow diffusion of methanol into a dichloromethane solution of the compound. The crystallographically determined structure of **4** shows that it is the α-1-α regioisomer, with the hydrogen atoms at the C2 of the pyrrolidine ring in an *endo-exo* orientation (Fig. 7b). This molecule also crystallizes in a centrosymmetric space group with one entire molecule in the asymmetric unit. Compound **4** is also a chiral molecule. The crystal consists of a racemic mixture (*RR* and *SS*), similar to the situation observed for **3** and the related C_{60} adduct (compound **C**, Fig. 2a) [31].

Interestingly, comparing the regioisomers obtained for the *bis*-1,3-dipolar cycloadditions with those obtained for the *bis*-diazo [31] and *bis*-Bingel [38] cycloadditions on C_{70}, we observed a remarkable difference in the reactivity of the inequivalent [6,6]-junctions depending on the type of cycloaddition reaction performed. For the case of the *bis*-diazo cycloaddition to C_{70}, the α-1-α regioisomer was the major product [31], showing that the isomers

Table 1
Selected bond distances in the adducts.

	α-bond length (Å)	β-bond length (Å)
Free C_{70}	1.375 (average)	1.387 (average)
β-2-β (**1**)	**1.337(2)**, 1.3804(17), 1.3945(17)	**1.5662(15)**, 1.3928(17), 1.387(3)
	*1.395(3), 1.3933(19), 1.3905(19)	*1.3845(18), 1.3863(18), 1.386(3)
α-1-β (**3**)	**1.586(6)**, 1.362(7), 1.391(7), 1.394(8), 1.369(8)	1.382(7), **1.570(7)**, 1.379(7), 1.381(9), 1.374(8)
	*1.408(8), 1.381(8), 1.354(8), 1.355(8), 1.409(9)	*1.346(9), 1.406(9), 1.358(8), 1.361(8), 1.361(8)
α-1-α (**4**)	**1.558(8)**, **1.583(8)**, 1.384(9), 1.404(8), 1.379(8)	1.393(9), 1.372(9), 1.334(9), 1.362(9), 1.367(9)
	*1.392(10), 1.376(10), 1.403(11), 1.392(11), 1.403(10)	*1.399(11), 1.352(11), 1.367(11), 1.383(10), 1.372(10)

Distances in boldface are the C–C bond lengths at the sites of addition, the * indicates the corresponding distances involving the C–C bonds in the opposite end cap where no addition has occurred.

Fig. 7. Crystallographically determined structure of **a**) compound **3** (α-1-β *endo-exo*) and **b**) compound **4** (α-1-α *endo-exo*). The apical pentagons of C_{70} are shown in pink, the carbon atoms of the pyrrolidine rings attached to the α-bonds are red and those carbons atoms attached to the β-bonds are yellow. Nitrogen atoms are blue. For clarity hydrogen atoms have been omitted except for the hydrogen atoms on C2 of the pyrrolidine ring. Thermal ellipsoids are drawn at the 0.50 level. (A colour version of this figure can be viewed online.)

Table 2
Redox Potentials[a] and UV/vis absorption maxima of **1** and **2**.

Compound	$E^{0/-}$	$E^{-/-2}$	$E^{-2/-3}$	UV/vis (toluene)
C_{70} [31]	−0.98	−1.31	−1.75	323, 369, 470, 542 (sh) [39]
β-2-β (**1**)	−1.37	−1.72	−2.21	353, 390, 434 (sh), 480, 635
α-2-α (**2**)	−1.38	−1.74	−2.16	393 (sh), 414 (sh), 425, 454 (sh), 503, 569, 713

[a] Values obtained by square wave voltammetry (SWV) in volts vs Fc/Fc$^+$ couple. sh = shoulder.

observed for this type of reaction are those formed from the addition at the more reactive α-bonds (kinetic control). Similar results were observed for the *bis*-Bingel cycloaddition to C_{70}, in which the length and rigidity of the *bis*-tether linker and the higher reactivity of the α-bonds directed the formation of a dumbbell-C_{70} as the major product (kinetic control).

Although one should not make direct comparisons between three different reactions that proceed through different mechanisms, the 1,3-dipolar, *bis*-diazo and *bis*-Bingel cycloadditions preferentially attack the α- and β-bonds. This observation shows the remarkable difference in the reactivity of α- and β-bonds compared with the γ- and δ-bonds, and provides the challenge of looking for reactions able to afford the unexplored γ- and δ-isomers.

3.3. Electrochemical studies of symmetric bis-pyrrolidines C_{70} **1** and **2**

The electrochemical properties of **1** and **2** were measured by cyclic voltammetry (CV) and SWV on a glassy carbon minielectrode with *ortho*-dichlorobenzene (*o*-DCB) as solvent and *n*-Bu$_4$NPF$_6$ as supporting electrolyte. The reduction potentials are shown in Table 2. As expected, the reduction potentials of **1** and **2** are cathodically shifted with respect to the values of pristine fullerene C_{70} by approximately 400 mV [40].

4. Conclusions

We described the one step synthesis of four, easily isolable, *bis*-pyrrolidine adducts of C_{70}. In addition, we unambiguously assigned these four [70]fullerene *bis*-adducts as the α-2-α, β-2-β, α-1-β and α-1-α regioisomers. These results substantially enrich the library of well-characterized [70]fullerene *bis*-adducts and also contribute to the understanding of the reactivity of the higher fullerenes. These compounds represent rare examples of *bis*-adducts of C_{70} in which

both addends are positioned on the same hemispherical pole of the fullerene.

Based on our observations, we can propose that the 1,3-dipolar cycloaddition reaction of azomethine ylides on C_{70} is primarily controlled by the optimal conformation adopted by the dipole, with two bonds between the two pyrrolidines, to obtain the unexpected α-2-α and β-2-β isomers, rather than controlled by the reactivity of the bonds on the carbon cage, which would have led to the formation of the α-1-α regioisomer as one of the main products.

We also note that all four [70]fullerene *bis*-adducts possess higher absorption coefficients when compared with the [60] fullerene *bis*-adducts analogs, suggesting better acceptor properties if used in OPV solar cells.

Acknowledgments

Appendix A. Supplementary data

Supplementary data related to this article can be found at http://dx.doi.org/10.1016/j.carbon.2016.04.044.

References

[1] C.L. Chochos, N. Tagmatarchis, V.G. Gregoriou, Rational design on n-type organic materials for high performance organic photovoltaics, RSC Adv. 3 (2013) 7160—7181.

[2] A. Mishra, P. Bäuerle, Small molecule organic semiconductors on the move: promises for future solar energy technology, Angew. Chem. Int. Ed. 51 (2012) 2020—2067.

[3] D.M. Guldi, Fullerenes: three dimensional electron acceptor materials, Chem.

Commun. (2000) 321–327.

[4] T. Mikie, A. Saeki, N. Ikuma, K. Kokubo, S. Seki, Hetero bis-addition of spiro-acetalized or cyclohexanone ring to 58π fullerene impacts solubility and mobility balance in polymer solar cells, ACS Appl. Mater. Interfaces 7 (2015) 12894–12902.

[5] D. Baran, S. Erten-Ela, A. Kratzer, T. Ameri, C.J. Brabec, A. Hirsch, Facile synthesis and photovoltaic applications of a new alkylated bismethano fullerene as electron acceptor for high open circuit voltage solar cells, RSC Adv. 5 (2015) 64724–64730.

[6] X. Meng, W. Zhang, Z a Tan, C. Du, C. Li, Z. Bo, et al., Dihydronaphthyl-based [60]fullerene bisadducts for efficient and stable polymer solar cells, Chem. Commun. 48 (2012) 425–427.

[7] B. Zhang, J. Subbiah, Y.-Y. Lai, J.M. White, D.J. Jones, W.W.H. Wong, One-pot selective synthesis of a fullerene bisadduct for organic solar cell applications, Chem. Commun. 51 (2015) 9837–9840.

[8] L. Lu, T. Zheng, Q. Wu, A.M. Schneider, D. Zhao, L. Yu, Recent Advances in Bulk Heterojunction Polymer Solar Cells, Chem. Rev. 115 (2015) 12666–12731.

[9] W.W.H. Wong, J. Subbiah, J.M. White, H. Seyler, B. Zhang, D.J. Jones, et al., Single isomer of indene-C_{70} bisadduct—isolation and performance in bulk heterojunction solar cells, Chem. Mater. 26 (2014) 1686–1689.

[10] K. Sun, Z. Xiao, S. Lu, W. Zajaczkowski, W. Pisula, E. Hanssen, et al., A molecular nematic liquid crystalline material for high-performance organic photovoltaics, Nat. Commun. 6 (2015).

[11] R. Tao, T. Umeyama, T. Higashino, T. Koganezawa, H. Imahori, Synthesis and isolation of cis-2 regiospecific ethylene-tethered indene dimer–[70]fullerene adduct for polymer solar cell applications, ACS Appl. Mater. Interfaces 7 (2015) 16676–16685.

[12] R.K.M. Bouwer, G.-J.A.H. Wetzelaer, P.W.M. Blom, J.C. Hummelen, Influence of the isomeric composition of the acceptor on the performance of organic bulk heterojunction P3HT:bis-PCBM solar cells, J. Mater. Chem. 22 (2012) 15412–15417.

[13] L. Hu, R. Cui, H. Huang, G. Lin, X. Guo, S. Yang, et al., Isomers of $IC_{70}BA$ and their photovoltaic performance in polymer solar cells, J. Nanosci. Nanotechnol. 15 (2015) 5285–5290.

[14] X. Meng, G. Zhao, Q. Xu, Z a Tan, Z. Zhang, L. Jiang, et al., Effects of fullerene bisadduct regioisomers on photovoltaic performance, Adv. Funct. Mater. 24 (2014) 158–163.

[15] R. Tao, T. Umeyama, T. Higashino, T. Koganezawa, H. Imahori, A single cis-2 regioisomer of ethylene-tethered indene dimer-fullerene adduct as an electron-acceptor in polymer solar cells, Chem. Commun. 51 (2015) 8233–8236.

[16] K. Kordatos, S. Bosi, T. Da Ros, A. Zambon, V. Lucchini, M. Prato, Isolation and characterization of all eight bisadducts of fulleropyrrolidine derivatives, J. Org. Chem. 66 (2001) 2802–2808.

[17] L. Isaacs, R.F. Haldimann, F. Diederich, Tether-directed remote functionalization of buckminsterfullerene: regiospecific hexaadduct formation, Angew. Chem. Int. Ed. 33 (1994) 2339–2342.

[18] S. Sergeyev, F. Diederich, Regio- and stereoselective tether-directed remote functionalization of C60 with derivatives of the Tröger base, Angew. Chem. Int. Ed. 43 (2004) 1738–1740.

[19] C. Thilgen, S. Sergeyev, F. Diederich, Spacer-controlled multiple functionalization of fullerenes, Top. Curr. Chem. 248 (2005) 1–61.

[20] C. Thilgen, F. Diederich, Structural aspects of fullerene chemistry a journey through fullerene chirality, Chem. Rev. 106 (2006) 5049–5135.

[21] C. Thilgen, F. Diederich, Tether-directed remote functionalization of fullerenes C_{60} and C_{70}, C. R. Chim. 9 (2006) 868–880.

[22] E.E. Maroto, A. de Cózar, S. Filippone, Á. Martín-Domenech, M. Suarez, F.P. Cossío, et al., Hierarchical selectivity in fullerenes: site-, regio-, diastereo-,

and enantiocontrol of the 1,3-dipolar cycloaddition to C70, Angew. Chem. Int. Ed. 50 (2011) 6060–6064.

[23] S. Vidal, M. Izquierdo, S. Filippone, F.G. Brunetti, N. Martin, Reaction of diazocompounds with C70: unprecedented synthesis and characterization of isomeric [5,6]-fulleroids, Chem. Commun. 51 (2015) 16774–16777.

[24] S.R. Wilson, Q. Lu, 1,3-dipolar cycloaddition of N-methylazomethine ylide to C_{70}, J. Org. Chem. 60 (1995) 6496–6498.

[25] F. Langa, P. de la Cruz, A. de la Hoz, E. Espíldora, F.P. Cossío, B. Lecea, Modification of regioselectivity in cycloadditions to C70 under microwave irradiation, J. Org. Chem. 65 (2000) 2499–2507.

[26] B. Jin, R.-F. Peng, J. Shen, G.-W. Wang, B.-S. Tan, S.-J. Chu, Direct formation of cycloadducts between fullerenes and amino acids through electron-transfer processes, Synth. Commun. 42 (2012) 1532–1541.

[27] P.A. Troshin, A.S. Peregudov, S.I. Troyanov, R.N. Lyubovskaya, New pyrrolidine and pyrroline derivatives of fullerenes: from the synthesis to the use in light-converting systems, Russ. Chem. Bull. 57 (2008) 887–912.

[28] P.A. Troshin, A.S. Peregudov, S.M. Peregudova, R.N. Lyubovskaya, Highly regio-and stereoselective [2+3] cycloadditions of azomethine ylides to [70] fullerene, Eur. J. Org. Chem. 2007 (2007) 5861–5866.

[29] M. Izquierdo, M.R. Cerón, N. Alegret, A.J. Metta-Magana, A. Rodriguez-Fortea, J.M. Poblet, et al., Unexpected isomerism in cis-2 bis(pyrrolidino)[60]fullerene diastereomers, Angew. Chem. Int. Ed. 52 (2013) 12928–12931.

[30] Z. Da-Gui, L. Yu-Liang, F. Lou-Zhen, L. Feng-Ying, L. Yong-Fanga, Z. Dao-Ben, 1,3-Dipolar cycloaddition reaction of two different azomethine ylides to C70, Chin. J. Chem. 16 (1998) 178–183.

[31] M.R. Cerón, M. Izquierdo, A. Aghabali, J.A. Valdez, K.B. Ghiassi, M.M. Olmstead, et al., Tethered bisadducts of C_{60} and C_{70} with addends on a common hexagonal face and a 12-membered hole in the fullerene cage, J. Am. Chem. Soc. 137 (2015) 7502–7508.

[32] M. Urbani, B. Pelado, P. de la Cruz, K-i Yamanaka, O. Ito, F. Langa, Synthesis and photoinduced energy- and electron-transfer processes of C60–oligothienylenevinylene–C70 dumbbell compounds, Chem. Eur. J. 17 (2011) 5432–5444.

[33] L. Ni, W.-W. Yang, Z.-J. Li, D. Wu, X. Gao, Regioselective oxazolination of C_{70}^{2-} and formation of cis-1 C_{70} adduct with respect to the apical pentagon, J. Org. Chem. 77 (2012) 7299–7306.

[34] M. Sander, T. Jarrosson, S.-C. Chuang, S.I. Khan, Y. Rubin, Approaches to open fullerenes: synthesis and thermal stability of cis-1 bis(isobenzofuran) Diels–Alder adducts of C_{60}, J. Org. Chem. 72 (2007) 2724–2731.

[35] M.D. Tzirakis, M.N. Alberti, M. Orfanopoulos, Photocycloaddition of biscyclopropyl alkenes to C_{60}: an unprecedented approach toward cis-1 tricyclic-fused fullerenes, Org. Lett. 13 (2011) 3364–3367.

[36] M.J. van Eis, P. Seiler, L.A. Muslinkina, M. Badertscher, E. Pretsch, F. Diederich, et al., Supramolecular fullerene chemistry: a comprehensive study of cyclophane-type mono- and bis-crown ether conjugates of C70, Helv. Chim. Acta 85 (2002) 2009–2055.

[37] V.S. Neti, M.R. Cerón, A. Duarte-Ruiz, M.M. Olmstead, A.L. Balch, L. Echegoyen, High-yield, regiospecific bis-functionalization of C70 using a Diels-Alder reaction in molten anthracene, Chem. Commun. 50 (2014) 10584–10587.

[38] M.R. Cerón, M. Izquierdo, Y. Pi, S.L. Atehortúa, L. Echegoyen, Tether-directed bisfunctionalization reactions of C_{60} and C_{70}, Chem. Eur. J. 21 (2015) 7881–7885.

[39] B. Li, C. Shu, X. Lu, L. Dunsch, Z. Chen, T.J.S. Dennis, et al., Addition of carbene to the equator of C_{70} to produce the most stable $C_{71}H_2$ isomer: 2 aH-2(12)a-homo(C_{70}-D_{5h}(6))[5,6]fullerene, Angew. Chem. Int. Ed. 49 (2010) 962–966.

[40] M. Lenes, G.-J.A.H. Wetzelaer, F.B. Kooistra, S.C. Veenstra, J.C. Hummelen, P.W.M. Blom, Fullerene bisadducts for enhanced open-circuit voltages and efficiencies in polymer solar cells, Adv. Mater. 20 (2008) 2116–2119.